

HYALURONAN-BASED PERICELLULAR MATRIX: SUBSTRATE ELECTROSTATIC CHARGES AND EARLY CELL ADHESION EVENTS

Caterina Fotia¹, Grazia M.L. Messina³, Giovanni Marletta³, Nicola Baldini^{1,2} and Gabriela Ciapetti^{1,*}

¹SSD Laboratory of Orthopaedic Pathophysiology and Regenerative Medicine, Istituto Ortopedico Rizzoli, Bologna, Italy

²Department of Biomedical and Neuromotor Sciences, University of Bologna, Bologna, Italy

³Laboratory for Molecular Surfaces and Nanotechnology (LAMSUN), Department of Chemical Sciences, University of Catania and CSGI, Catania, Italy

Abstract

Cells are surrounded by a hyaluronan-rich coat called 'pericellular matrix' (PCM), mainly constituted by hyaluronan, a long-chain linear polysaccharide which is secreted and resorbed by the cell, depending on its activity. Cell attachment to a surface is mediated by PCM before integrins and focal adhesions are involved. As hyaluronan is known to bear a negative charge at physiological pH, the relevance of its electrical properties in driving the early cell adhesion steps has been studied, exploring how PCM mediates cell adhesion to charged surfaces, such as polyelectrolyte multilayer (PEM) films. Poly(ethylene imine) (PEI) and poly(sodium 4-styrene sulphonate) (PSS), assembled as PEI/PSS and PEI/PSS/PEI layers, were used. The nanoscale morphology of such layers was analysed by atomic force microscopy, and the detailed surface structure was analysed by X-ray photoemission spectroscopy. PCM-coated and PCM-depleted MG63 osteoblast-like cells were used, and cell density, morphology and adhesive structures were analysed during early steps of cell attachment to the PEM surfaces (1-6 h). The present study demonstrates that the pericellular matrix is involved in cell adhesion to material surfaces, and its arrangement depends on the cell interaction with the surface. Moreover, the PCM/surface interaction is not simply driven by electrostatic effects, as the cell response may be affected by specific chemical groups at the material surface. In the development of biomimetic surfaces promoting cell adhesion and function, the role of this unrecognised outer cell structure has to be taken into account.

Keywords: Pericellular matrix; hyaluronan; cell adhesion; polyelectrolyte multilayers.

*Address for correspondence:

Dr Gabriela Ciapetti
SSD Laboratory of Orthopaedic Pathophysiology and Regenerative Medicine
Istituto Ortopedico Rizzoli
via di Barbiano 1/10
40136 Bologna, Italy

Telephone Number: +390516366897

FAX Number: +390516366748

E-mail: gabriela.ciapetti@ior.it

Introduction

Cell adhesion to extracellular matrix or foreign substrates is mediated by a hyaluronan-based coat, the so-called pericellular matrix (PCM), with defined morphological, biochemical, and biomechanical features (Zimmerman *et al.*, 2002; Lee *et al.*, 1993; Knudson and Knudson, 1993). This hydrophilic layer, featuring anti-adhesive properties, interposes between the plasma membrane and the nearby surfaces (Entwistle *et al.*, 1996).

Hyaluronic acid is a non-sulphated glycosaminoglycan, composed of D-glucuronic acid and D-glucosamine, that is negatively charged under physiological conditions. Hyaluronan synthesis and deposition change depending on cell activities, such as cell growth, confluence, mitosis, or detachment from a substrate, and is modulated by calcium or lactate concentration, pO₂, viral transformation, and serum (Stern, 2003).

All living cells are coated with this polysaccharide-rich layer of widely varying thickness, ranging between a few tenths of a μm and several μm . The large size of the PCM mediates the range of cell interactions with substrates, when the cell membrane is still far from the adhesive surface, well before integrin-mediated focal adhesions are effective (Cohen *et al.*, 2004). In a time-frame of ms following such interaction, cell adherence to substrates occurs, in turn followed by cytoskeletal reorganisation and activation of signalling cascades that are responsible for cell spreading, migration, proliferation, differentiation, and survival (Bigerelle and Anselme, 2005). PCM is therefore likely to regulate cell adhesion to any surface, including biomaterials and tissue engineering scaffolds, before the formation of integrin-mediated focal adhesion complexes.

At a nanoscale level, an additional role of PCM is the interplay of electrical charges of hyaluronan chains with those present on substrate surfaces, where protonation/de-protonation of specific functional groups are present (Finke *et al.*, 2007). In this paper, the response of cells, with and without PCM, to biomaterials with a controlled chemical structure and electrical charge was analysed in order to explore the relevance of the hyaluronan-based PCM and its electrical properties in cell adhesion. To this purpose, self-assembling films of polyelectrolyte multilayers (PEM) were chosen to evaluate cell reactions to a well-defined charged surface. PEM are built-up using a layer-by-layer deposition method based on electrostatic interactions, with the assembly of polyanion/polycation constituting a layer pair. The tunability of PEM provides

a unique opportunity to mimic the complex *in vivo* extracellular matrix environment. In this study cationic poly(ethylene imine) (PEI) and anionic poly(sodium 4-styrene sulphonate) (PSS) have been used. PEI may exert some cytotoxicity when used at high concentration, such as 5 mg/mL, but at lower concentration, i.e. 2 mg/mL, adhesion and proliferation of cells is undisturbed (Tryoen-Tóth *et al.*, 2002; Brunot *et al.*, 2007; Niepel *et al.*, 2011). PSS was found to be biologically accepted when used at 1 mg/mL or 5 mg/mL (Ting *et al.*, 2010; Tryoen-Tóth *et al.*, 2002). Based on these previous reports, we selected low concentrations that have been described to be non-toxic.

In this study, MG63 osteoblast-like cells were seeded on two polyelectrolyte films with opposite electric charge to further define the role of PCM in the early phases of cell adhesion to synthetic substrates, with particular reference to the role of electrostatic interactions at the nanoscale level.

Materials and Methods

Polyelectrolyte multilayers

Polyelectrolyte solutions were prepared as follows: cationic poly(ethylene imine) (PEI, MW 750,000) and anionic poly(sodium 4-styrene sulphonate) (PSS, MW 70,000) were purchased from Sigma, and dissolved in ultrapure Millipore water. Solutions of PEI ($pK_{a(\text{app})} \sim 8.8$) and PSS ($pK_{a(\text{app})} \sim 2.1$) were prepared in Millipore water at a concentration of 1 mg/mL and pH 8.8 and 6.4, respectively. Simple immersion in the PEI or PSS solutions for 15 min were enough to achieve a complete layer of each polyelectrolyte: PEM were built-up on glass chamber slides by alternating PEI and PSS layer deposition to get a ~ 3.0 nm thick PEI-PSS film with an anionic surface, and a 4.5 nm thick PEI-PSS-PEI film with a cationic surface.

Before polyelectrolyte deposition, glass surfaces were irradiated with UV-O3 for 30 min at atmospheric pressure in a Jelight Instruments apparatus (λ_{ex} of 185 and 254 nm) to remove any carbon moiety, washed extensively with ultrapure water and dried with blown nitrogen.

For clarity, the cell-facing outer layer is used throughout the text as a shorthand for multilayers, with PEI indicating the PEI/PSS/PEI multilayer, and PSS for the PEI/PSS multilayer.

AFM analysis

Atomic force microscopy (AFM) was applied using a Nanoscope IIIA-MultiMode AFM (Digital Instruments, Santa Barbara, CA, USA) with a “J scanner” in tapping mode under ambient conditions. The force was maintained at the lowest possible value by continuous adjusting the set point during imaging. Images were recorded using 0.005–0.02 $\Omega \cdot \text{m}$ phosphorous (n)-doped silicon tips mounted on cantilevers with a nominal force constant of 40 N/m and a resonance frequency of 300 kHz.

XPS analysis

Angular-dependent X-ray photoelectron spectroscopy (AD-XPS) with a small spot apparatus (Axis-Ultra, Kratos Analytical Ltd, Manchester, UK), equipped

with hemispherical analyser, was used to acquire both compositional survey and detailed scans.

The XPS measurements have been performed in Angular Dependent mode. That is, by exploiting the change in the depth analysed by changing the angle of photoelectron take-off. Setting the take-off angles at 0° (normal incidence, sampling depth ~ 10 nm) and 70° (surface-enhanced incidence, sampling depth ~ 3.4 nm) with respect to the normal axis to the sample surface, the concentration from the bulk to the outer film surface can be measured (Briggs and Seah, 1990). Thus, the estimated thickness are 9.4 nm at 0° and 4.7 nm at 70° take-off angles (θ), respectively (Popat *et al.*, 2004). In order to avoid any damage to the sample during the data acquisition, the X-ray source (Al $K\alpha_{1/2}$) was used at a reduced power of 15 kV and 10 mA, with a $\leq 1.33 \times 10^{-6}$ Pa pressure. All binding energies were referenced to the C 1s neutral carbon peak at 284.6 eV (Suzuki *et al.*, 1988). The Shirley-type background was subtracted from each spectrum. The peak fitting analysis was performed using the XPS-PEAK41 software and Gaussian curves, with constant full width at half-maximum for all the components of a given peak.

Preparation of control substrates

Human fibronectin (Sigma-Aldrich, Milan, Italy) was prepared at 0.1 mg/mL in MilliQ water and kept at room temperature for 30 min. Human type I collagen (Sigma) was dissolved at 1 mg/mL in 0.1 M acetic acid (pH 3) at room temperature for 60 min. Both proteins were diluted to 5 $\mu\text{g/mL}$ in phosphate-buffered saline (PBS), and used to coat the glass plates (Nalgene Nunc, Roskilde, Denmark) by overnight incubation at 4°C .

Cell culture and seeding

MG63 cells were grown in Iscove's Modified Dulbecco's Medium (IMDM, Invitrogen, Carlsbad, CA) supplemented with 10 % foetal bovine serum (FBS, Mascia Brunelli, Milan, Italy), 2 mM L-glutamine, 100 U/mL penicillin and 0.1 mg/mL streptomycin (Invitrogen) in a humidified 5 % CO_2 atmosphere at 37°C .

Cells from 80 % confluent cultures were collected with 0.5 % trypsin-EDTA (Invitrogen) and seeded on PEM, Permanox[®], fibronectin or type I collagen at a density of 2.5×10^4 per cm^2 . To remove the pericellular matrix, MG63 cells were treated with 5 U/mL *Streptomyces* hyaluronidase (Sigma) in complete medium for 15 min and then plated on the different substrates with 2 U/mL hyaluronidase-added medium, to avoid new hyaluronan secretion. For clarity, the prefix ‘hyal’ is used onward for cells deprived of pericellular matrix.

Cell transfection with GFP

MG63 cells were cultured with antibiotic-free medium for 24 h, then transfected using Neon[™] Transfection System Kit (Invitrogen). Briefly, 0.5 μg of plasmid DNA with green fluorescent protein (GFP) were added to 5×10^5 cells resuspended in buffer. Following cell microporation (three pulses 1300V/10 ms, Microporator MP-100, Digital Bio Technology, Seoul, Korea), the cell suspension was seeded in a 6-well plate. After 48 h GFP-positive cells were detached and used in the experiment.

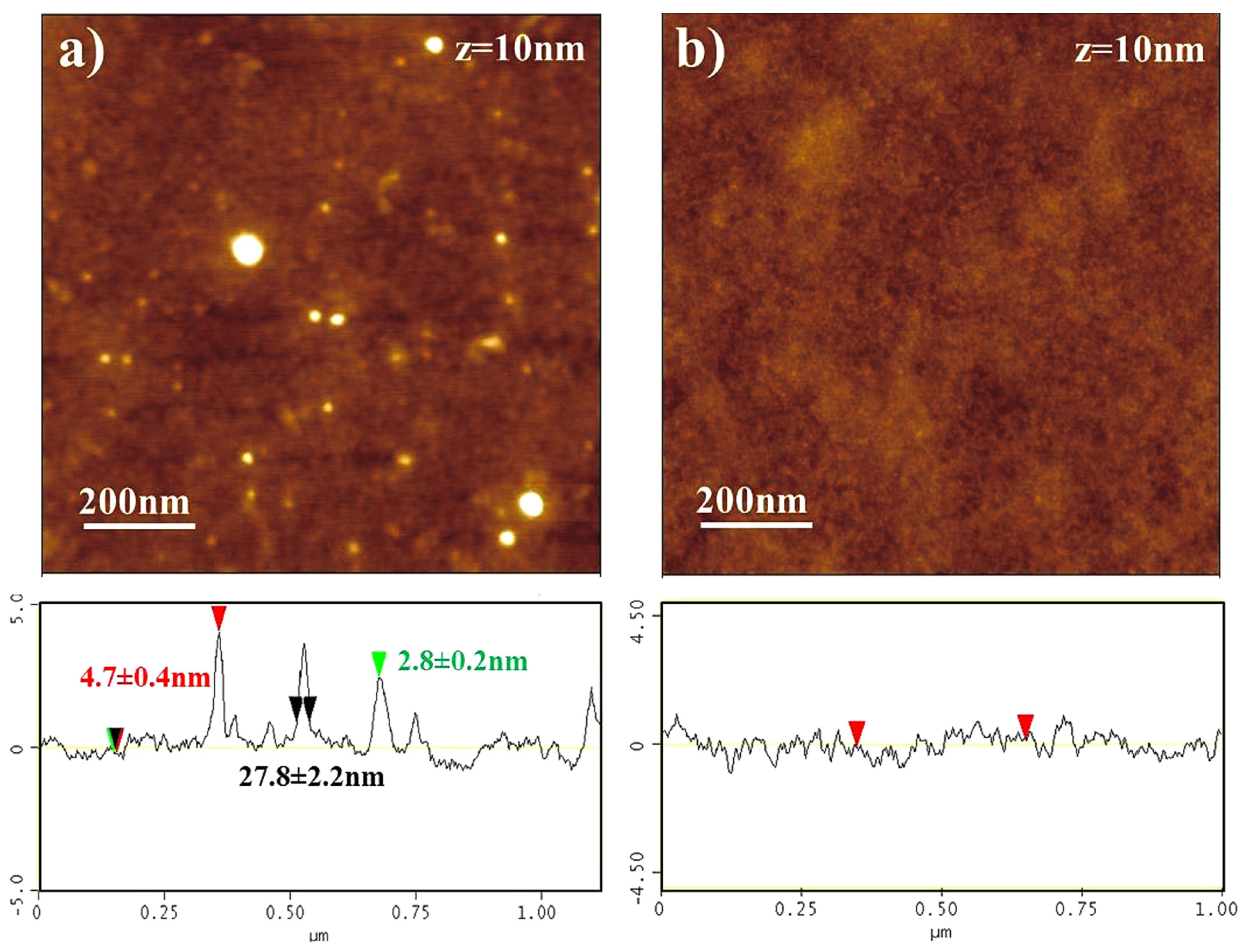


Fig. 1. AFM micrographs of different PEM films. Topography of (a) the PEI/PSS bilayer and (b) the PEI/PSS/PEI multilayers.

Erythrocyte exclusion test

Sheep red blood cells (Sigma), 1×10^7 , were added to MG63 cells at 3 h from seeding on 10 % FBS-coated glass coverslips, and time-lapse microscopy applied after 5 min.

Hyaluronan labelling

Following detachment using trypsin-EDTA, 2.5×10^4 GFP-transfected cells/cm² were seeded on the different substrates. After 30 min, GFP-positive cells were incubated with 2 μ g/mL biotinylated HA-binding protein (bHABP) (Seikagaku Corporation, Tokyo, Japan) for 2 h at 37 °C, washed with PBS, stained using 5 μ g/mL Streptavidin-Alexafluor 586 (Molecular Probes, Invitrogen) for 30 min at 37 °C, and immediately observed by confocal microscopy (Eclipse E600, Nikon, Tokyo, Japan). Images of the pericellular matrix (red) around GFP-positive cells (green) were acquired using a 60x objective and a high-resolution digital camera. bHABP-stained sample for each condition was treated with hyaluronidase, and the disappearance of the red layer taken as a confirmation.

Cell number and spreading

The cells were seeded in duplicate on the different substrates, and non-adherent cells were removed with PBS. After 1, 3 and 6 h, adherent cells were fixed with 3 % (w/v) paraformaldehyde plus 2 % saccharose in PBS, permeabilised using 0.5 % Triton X-100 in HEPES

buffer, and incubated with 0.5 % μ g/mL phalloidin-TRITC (Sigma) for 45 min in the dark, to stain cytoskeletal f-actin. Then cell nuclei were stained with Hoechst 33258, 10 min in the dark (Sigma). After three washes with PBS, the specimens were mounted in glycerol/PBS and observed with a fluorescence microscope (Nikon Eclipse E800, Nikon). The number of adherent cells was obtained by counting the nuclei in six non-overlapping fields with a 20x objective. To assess cell spreading, six images (20x magnification) were taken on each sample and analysed using a dedicated software (LUCIA Measurement, version 4.60, Nikon Instruments, Tokyo, Japan). Changes of colour intensity based upon the fluorescence signal per pixel were detected, and the fluorescent area on the total area visualised (135,000 mm² at 20x magnification) was calculated. The cell spreading was quantified by dividing the red fluorescent area/total area ratio for the number of cells.

Fluorescence microscopy of adhesive proteins

After 6 h from seeding on PEM and control substrates, MG63 cells were fixed and permeabilised as described above. Following incubation with 0.5 % bovine serum albumin (BSA) in PBS with 10 % FBS for 15 min at room temperature to block unspecific binding sites, the adhesive proteins were stained using a 1:400 mouse anti-vinculin (Sigma), 2 μ g/mL rabbit anti-paxillin, and 20 μ g/mL mouse

Table 1. Atomic composition (%) of polyelectrolyte multilayers for XPS spectra obtained at normal (0°) and surface-enhanced take-off angle (70°).

SAMPLES	N %	S %	PSS % at surface	PEI % at surface
PEI/PSS 0°	4.9 ± 0.5	1.8 ± 0.2	60 %	40 %
PEI/PSS 70°	6.7 ± 0.6	3.3 ± 0.3	66 %	34 %
PEI/PSS/PEI 0°	13.8 ± 1.4	1.1 ± 0.2	24 %	76 %
PEI/PSS/PEI 70°	22.3 ± 2.3	0.9 ± 0.2	15 %	85 %

anti-integrin $\beta 1$ antibodies (Santa Cruz Biotechnology, Inc., Heidelberg, Germany) in PBS + 0.2 % BSA and a fluorescein-conjugated secondary antibody. Cytoskeletal f-actin was stained as described above. Fluorescent images were acquired by confocal laser scanning microscopy.

Western blot analysis

Cells were seeded in 60 mm-plate coated with the different substrates, and after 6 h whole-cell proteins were extracted by cold lysis. Cells were washed twice with cold PBS, scraped off the culture dishes, and resuspended in RIPA (radio-immunoprecipitation assay) buffer supplemented with a protease-inhibitor cocktail (Roche, Milan, Italy). After 30 min incubation at 4 °C, the samples were centrifuged at 14,000 rpm for 20 min at 4 °C, and the supernatant containing the protein extract was analysed by standard SDS-PAGE, transferred onto nitrocellulose membranes, and probed with the appropriate antibodies (FAK, phospho-FAK (Tyr 576/577); alpha-tubulin, Santa Cruz Biotechnology). The bound primary antibodies were detected using an appropriate horseradish peroxidase-conjugated secondary antibody (anti-rabbit IgG or anti-mouse IgG, peroxidase-linked; Amersham, Little Chalfont, UK) and the relevant band was visualised using a chemiluminescence detection kit (ECL, GE Healthcare, Milan, Italy). The experiment was repeated twice.

Results

Surface characterisation of polyelectrolyte films

Morphology at the nanoscale

The PEI/PSS bilayers and the PEI/PSS/PEI multilayers were built by the layer-by-layer deposition method (see Materials and Methods). Fig. 1 shows the nanoscale morphology of the film surfaces as obtained by AFM in tapping mode.

Both films exhibited a quite uniform substrate coverage. In fact, the PEI/PSS surface showed a uniform distribution of large PEM granules with $R_q = 0.64 \pm 0.15$ nm, whereas the PEI/PSS/PEI surface consisted of a granular but smoother film, with $R_q = 0.39 \pm 0.04$ nm. Therefore, according to the literature, the very low values of R_q measured are not expected to significantly affect the adhesion and spreading of cells.

Surface chemical structure: XPS quantitative results

Table 1 reports the atomic percentage of sulphur and nitrogen in the two PEM films, respectively derived from the areas of the S 2p peak, assumed as the marker of the

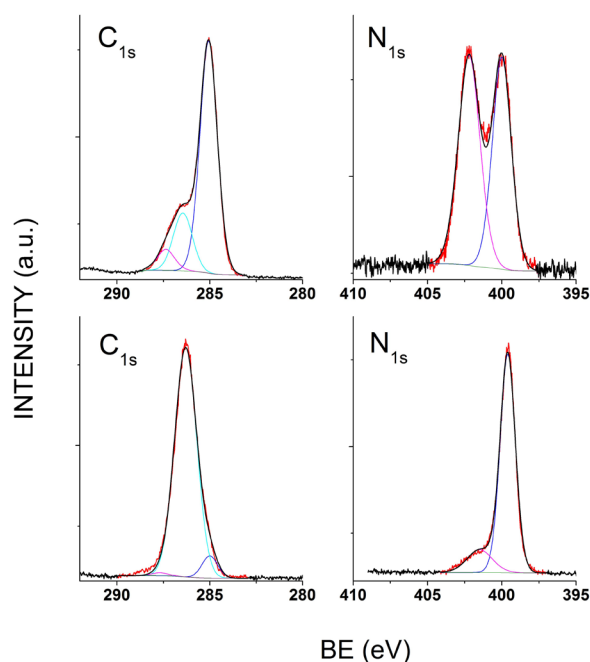


Fig. 2. C 1s and N 1s peaks from XPS spectra of the PEI/PSS film (top), and the PEI/PSS/PEI film (bottom).

PSS layer, and N 1s, assumed as the marker of the PEI layers. The data have been evaluated both for bulk-like and surface-enhanced conditions.

The comparison between the quantitative data reported in Table 1 for 0° and 70° XPS take-off angle for PEI/PSS film shows a marked increase (about 1.8 factor) at the surface of S signal, due to the $-\text{SO}_3^-$ groups of PSS, while the N signal (from the amine groups of PEI) increases only by about 1.3 times, confirming that the surface of the film is predominantly formed by the PSS layer. The signal from PEI is still relevant, due to the fact that under surface-enhanced mode the sampling depth is still about 3.4 nm, therefore sampling the whole ~3 nm-thick PEM film.

Likewise, the data reported in Table 1 for the PEI/PSS/PEI film show a huge increase of the N 1s peak (~1.6), and a slight decrease of the S 2p signal in surface-enhanced mode, indicating that the film surface is constituted by a PEI layer. In this case the sampling depth in surface-enhanced mode, ~3.4 nm, is slightly lower than the PEM film thickness (~4.5 nm).

Surface chemical structure: XPS peak shape analysis

Further hints on the structure of the films are derived from the analysis of the shape of the C 1s and N 1s peaks (Fig.

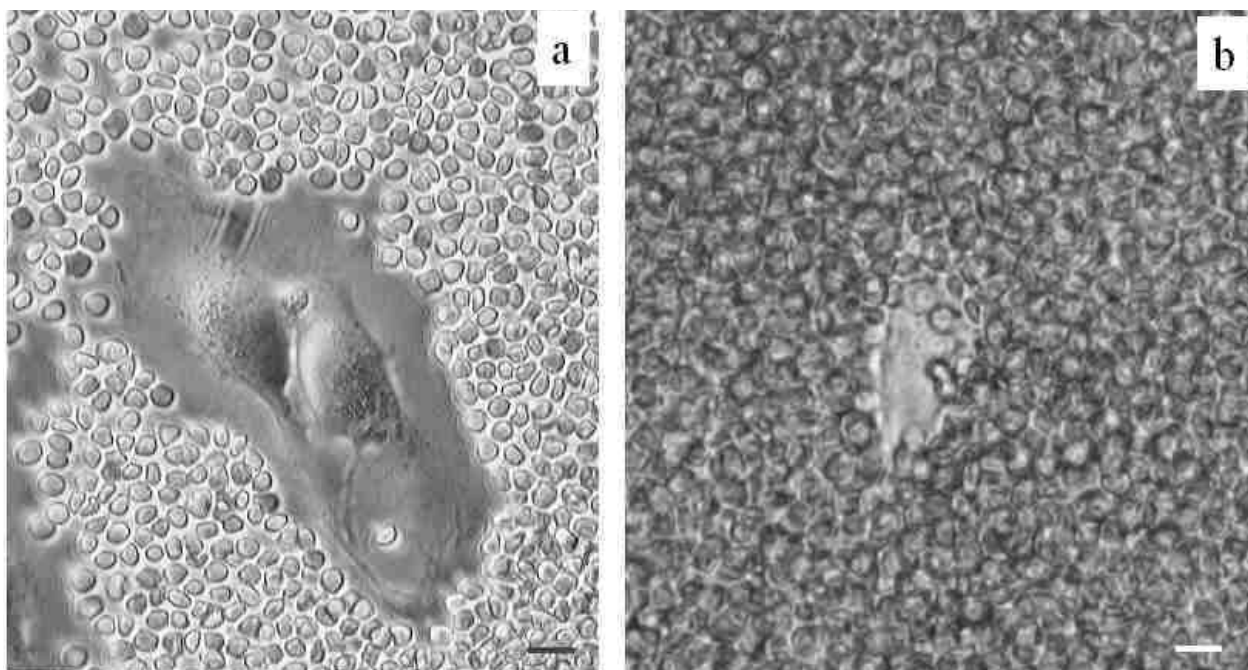


Fig. 3. Erythrocyte exclusion assay to visualise the pericellular matrix around MG63 cells. **(a)** PCM corresponds to the clear exclusion area between the cell and the fixed erythrocytes. **(b)** After treatment with hyaluronidase the PCM disappears, with red blood cells getting close to the cell profile. Bar = 20 μm .

2). Taking into account that the XPS sampling depth is higher than the film thickness for both PEI/PSS and PEI/PSS/PEI films, the XPS peaks recorded are a convolution of the signals originating from the whole film.

Thus, the C 1s peaks for both PEI/PSS and PEI/PSS/PEI films resulted from a convolution of the two components due to PSS, i.e., component 1 ($\sim 285.0 \pm 0.2$ eV) and 2 ($\sim 286.7 \pm 0.2$ eV), assigned to phenyl ring carbons and methylene groups, and to C-SO₃⁻ groups, respectively (Santos *et al.*, 2001), and the single component 3 (at 285.7 ± 0.2 eV) due to PEI, and assigned to the C-NH, C-NH₂ C-N groups in the PEI chains (Finšgar *et al.*, 2009).

Accordingly, the C 1s peak shape for PEI/PSS films is dominated by components 1 and 2, typical of the outer PSS layer, with a smaller contribution from the underlying PEI layer, while the C 1s peak in PEI/PSS/PEI films is dominated by component 3, characteristic of the outer PEI layers.

The N chemical state supported the above assignments, and provided further information on the chemical nature of the film surfaces, using the chemical state of the PEI film nitrogen as a marker of the interactions with PSS. Indeed, for the PEI/PSS films the N 1s peak is formed by two components of similar intensity, respectively due to quaternary nitrogen groups ($\sim 402.2 \pm 0.2$ eV binding energy (BE)), and to the backbone amine nitrogen (400.0 ± 0.2 eV BE) (Finšgar *et al.*, 2009). On the other hand, for the PEI/PSS/PEI films the N 1s peak was essentially formed by the component due to the amine groups (assigned to chain inside the PEI layer, not directly interacting with PSS chains), with a small quaternary nitrogen component, due to PEI chains at the interface with the PSS layer, where the positively charged quaternary nitrogen groups act as

counter-ions partially neutralising the negatively charged sulphonic groups.

Thus, we conclude that for PEI/PSS/PEI films the layer exposed to the biological medium is a homogeneous PEI layer covering the surface. At variance with this, for the PEI/PSS films, two potential structures are suggested: a layered structure with PSS lying onto PEI, with quaternary nitrogen at the very interface and an underlying layer of neutral PEI chains, or alternatively, an underlying PEI layer with a partially mixed layer of PSS and PEI.

Biological studies

Peri-cellular matrix evidention

The pericellular matrix of MG63 cells was seen using the erythrocyte exclusion assay. MG63 secreted a consistent pericellular matrix, seen as a red blood cell-free, clear, halo-like area surrounding the cell (Fig. 3a), which was removed after hyal-treatment (Fig. 3b). By time-lapse video microscopy, the kinetics of hyaluronan-coat formation around the cells was captured. Indeed, PCM formation is a rapid process; as already reported by Evanko *et al.* (1999), the cells synthesise a thick coat, and then resorb it in a few minutes (data not shown).

By confocal microscopy the pericellular matrix of the GFP-positive MG63 cells on PEI substrates was seen as a thick red border around the cells, which at 3 h keep a round shape (Fig. 4a). Following treatment with hyaluronidase, the cells were completely devoid of hyaluronan (Fig. 4b), and this has the effect of reducing the number of attached cells. On PSS films the cells tend to spread and elongate, showing a 'granular', irregular border of red hyaluronan. Their PCM was totally removed by hyaluronidase (Fig. 4c,d), with no evident effect on cell shape or number.

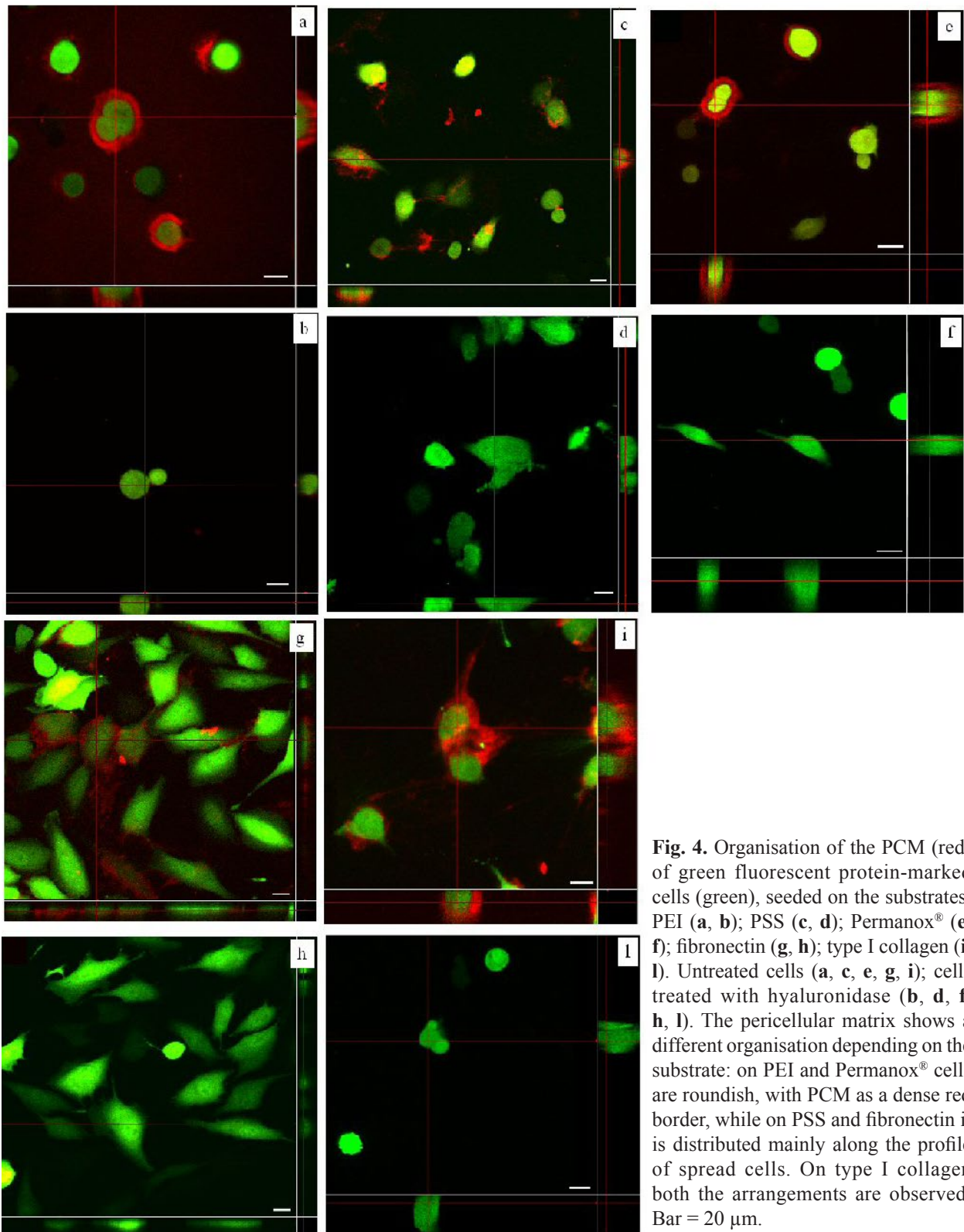


Fig. 4. Organisation of the PCM (red) of green fluorescent protein-marked cells (green), seeded on the substrates. PEI (**a, b**); PSS (**c, d**); Permanox® (**e, f**); fibronectin (**g, h**); type I collagen (**i, l**). Untreated cells (**a, c, e, g, i**); cells treated with hyaluronidase (**b, d, f, h, l**). The pericellular matrix shows a different organisation depending on the substrate: on PEI and Permanox® cells are roundish, with PCM as a dense red border, while on PSS and fibronectin it is distributed mainly along the profile of spread cells. On type I collagen both the arrangements are observed. Bar = 20 μ m.

On Permanox®, many cells were round, with a thick and homogeneous pericellular matrix, quite similar to that observed on PEI (Fig. 4e). Instead, the coat of MG63 cells seeded on fibronectin was similar to that observed for PSS: hyaluronan was only on a few spread cells and mainly distributed along the flanks of the cells (Fig. 4g). On collagen, some cells showed a strong continuous layer, while others had an irregular pericellular matrix (Fig. 4i).

Cell adhesion and spreading

The adhesion of MG63 cells to PEM and the other substrates was evaluated after 1, 3 and 6 h. Many cells adhered to PSS and PEI after 1 h, and no change was evident when cells were treated with hyaluronidase (Fig. 5). At 3 and 6 h from seeding, on PSS the cell density was only slightly lower with and without PCM, whereas on PEI the number of adherent cells was significantly

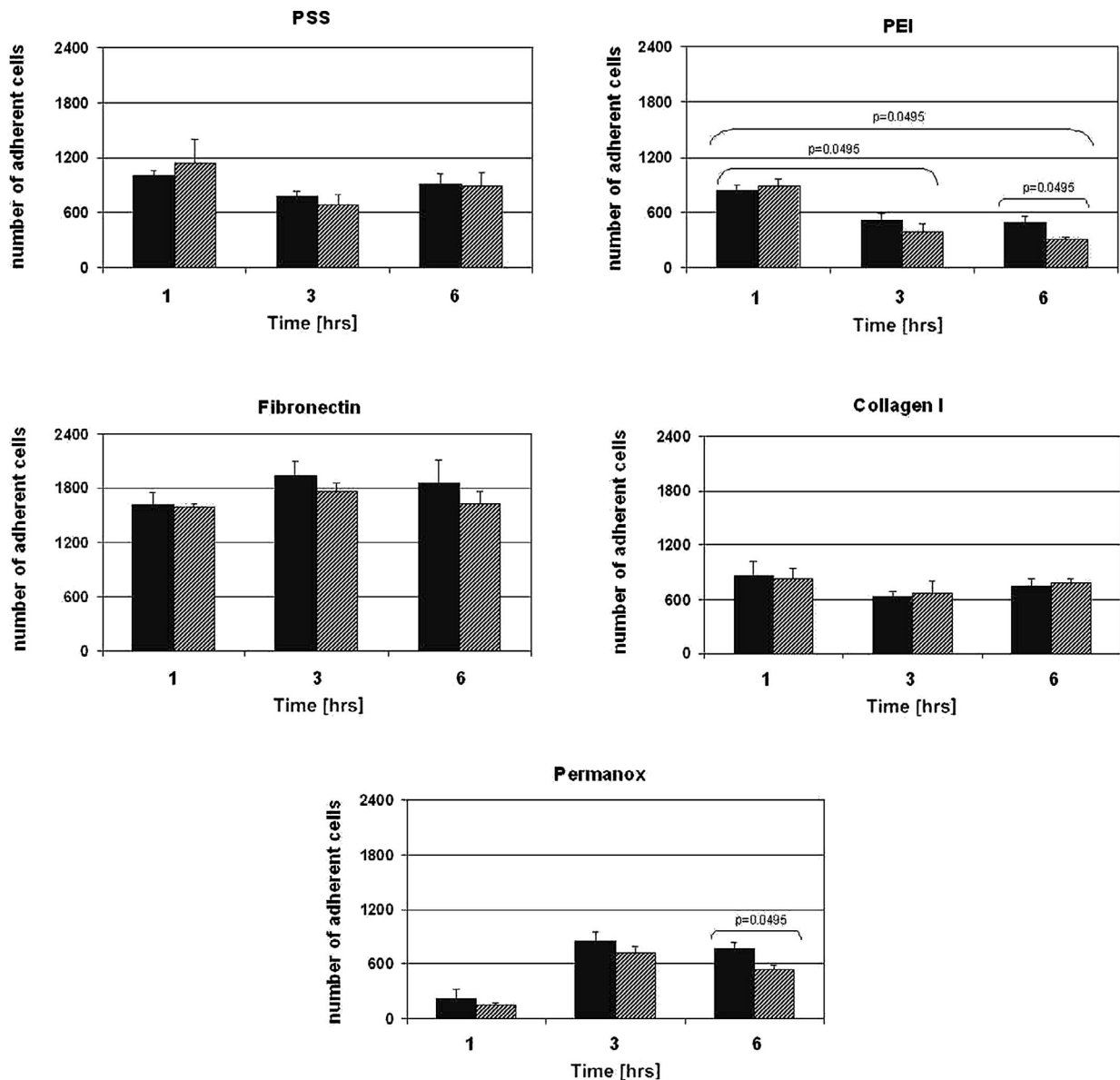


Fig. 5. Cell adhesion to the diverse substrates. MG63 were cultured on the different substrates for 1, 3 and 6 h. Nuclei were stained with Hoechst 33258 and adherent cells were counted. On PSS, fibronectin, and type I collagen the number of adherent cells does not change, also after hyaluronidase treatment. On PEI the number of cells slightly decreases with time, while on Permanox® cells adhere slowly. After treatment with hyaluronidase no change is recorded, except for PEI and Permanox at 6 h where the number of cells is decreased. Black bars, untreated cells; striped bars, hyaluronidase-treated cells. Mean \pm SEM.

reduced compared to the first time-point. Interestingly, the cells treated with hyal were less able to adhere to PEI with respect to untreated cells, with a significant difference at 6 h (untreated vs. hyal: $p = 0.0495$).

The highest cell adhesion was found on fibronectin, with or without hyal treatment, and the number of adherent cells increased over time (Fig. 5). As with PSS, many cells attached to collagen I at 1 h, with a small decrease observed at longer time-points. The slight decrease in the cell number on PSS and type I collagen at 3 h vs. 1 h is probably due to a slower adhesion process: many cells try to interact with the surface at 1 h, but not all the initial weak interactions mature to a stable adhesion. No difference was recorded with or without PCM. In contrast, on Permanox® the cells adhered weakly at 1 h, but after 3 h the number of adherent

cells was increased. Cells pre-treated with hyaluronidase adhered less compared to untreated cells, as on PEI, and the difference became significant after 6 h ($p < 0.05$ untreated vs. hyal).

By quantitative analysis of cell spreading, the cell area was shown to increase over time on all substrates, with the exception of PEI (Fig. 6). On PSS and fibronectin, the cells showed a well spread morphology already after 1 h, while on the other substrates the cells exhibited a roundish shape and covered only small areas. At later time-points, on collagen and Permanox®, the cells began to spread, showing a fully spread morphology at 6 h, while the cells on PEI kept a rounded shape with no increase in the area covered (Fig. 6).

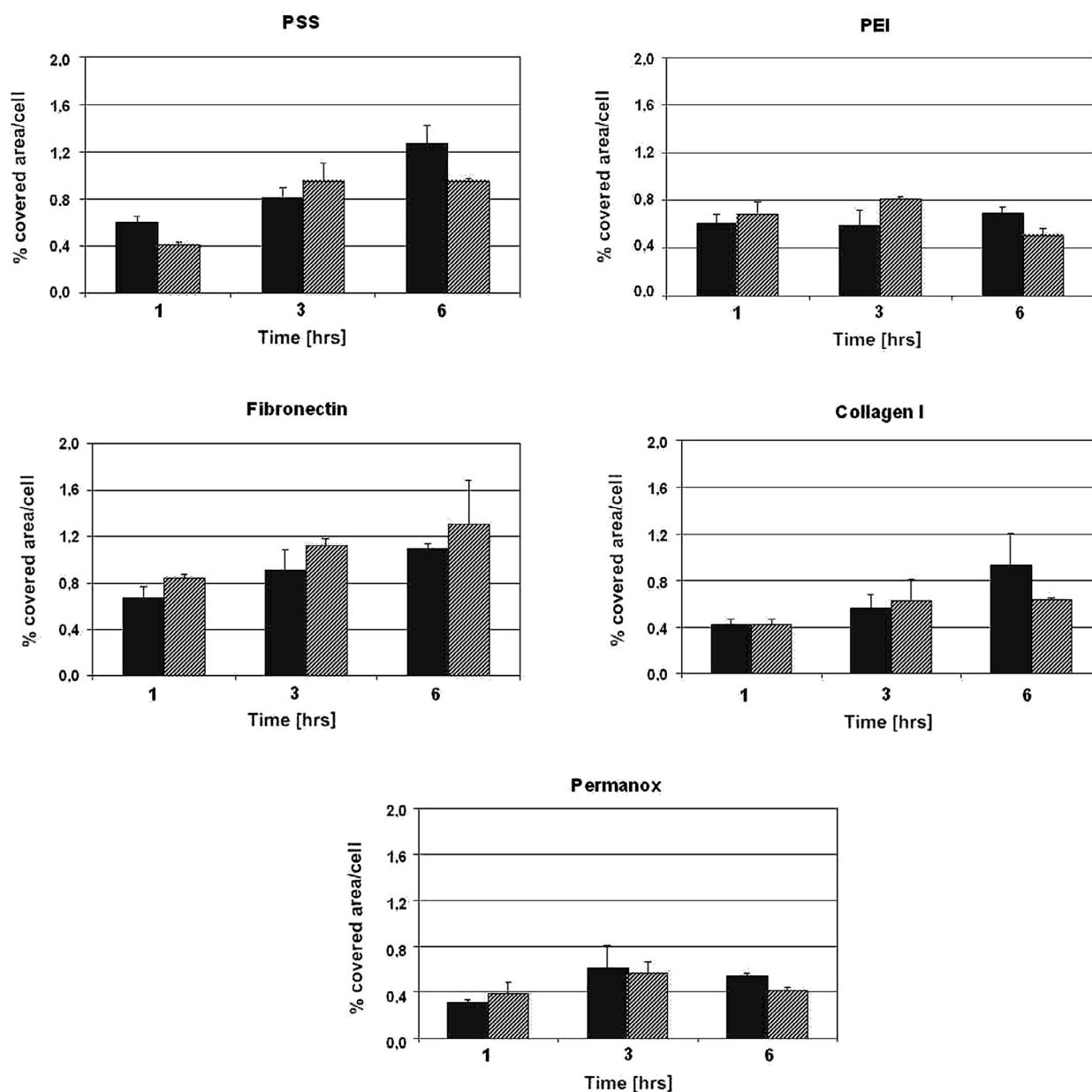


Fig. 6. Evaluation of cell spreading on the substrates. MG63 were cultured on the different substrates for 1, 3 and 6 h. The spreading was evaluated after staining cytoskeletal f-actin with phalloidin-TRITC. The area covered by cells increases over time on all substrates except on PEI, where cells maintain a round shape. Results are reported as mean \pm SEM of the fluorescent area of single cells. Black bars, untreated cells; striped bars, hyaluronidase-treated cells.

No remarkable differences were reported after hyal treatment compared to normal conditions for any of the substrates, but a tendency towards lower values of spreading was detected on PSS and PEI after 6 h.

Finally, cells cultured on PEI and PSS showed a different rate of migration by time-lapse microscopy: the cells on PEI were nearly immobilised on the surface, whereas cells on PSS were actively moving; such behaviour did not change after pericellular matrix removal (not shown).

Western blot analysis

The effect of the different substrates on the expression and activity of focal adhesion kinase (FAK) protein was

evaluated by western blot. FAK is a 125 kDa cytoplasmic tyrosine kinase widely expressed in the focal adhesion complex. The phosphorylated FAK activates several downstream signalling molecules implicated in integrin-mediated signalling pathways. These in turn are involved in cell adhesion, migration, and proliferation (Mitra *et al.*, 2005). As shown in Fig. 7, total and phospho-FAK levels were similar in both conditions for fibronectin, while a reduction was induced by PCM removal on the other substrates, especially for PEI, where FAK expression was strongly decreased. In Fig. 7, the ratio of phospho-FAK to total FAK band density, normalised on tubulin, is represented (two separate experiments). Activated FAK was high on fibronectin, while a two-fold decrease in FAK

activity was recorded on PEI, as compared to fibronectin. FAK activity on collagen and PSS was similar, and higher compared to PEI.

Cytoskeleton and focal contacts

The organisation of focal contacts on different substrates was analysed at 6 h after seeding, using immunocytochemical recognition of integrin $\beta 1$, paxillin and vinculin, and rhodamine-phalloidin for the cytoskeletal actin.

On PSS, MG63 cells were elongated, with actin stress-fibres tethered into focal adhesion contacts, where vinculin and paxillin were clearly visible and co-localised with actin. Integrin $\beta 1$ was present as a cytoplasmic pool (Fig. 8a,c,e). When cells were pre-treated with hyaluronidase, only few focal contacts formed. At the cell periphery paxillin was absent and vinculin diminished; moreover, no stress-fibres were seen (Fig. 8d,f).

Cells seeded on PEI were round in shape, and actin was seen as a cortical layer at the cell edge, filopodia and tips, without stress-fibres. The adhesion molecules did not organise into focal contacts, and were located centrally in the cell body. No change was detected when the pericellular matrix was removed (Fig. 9).

On Permanox[®], the cells were spread and actin was organised in fibres but, as on PEI, focal contacts were essentially missing, and vinculin was detected only in a few cells (Fig. 10e). This suggests the organisation of late focal complexes, which do not mature into focal adhesions. Removal of the pericellular matrix changed cell morphology and organisation, as many cells exhibited a roundish shape, with an undefined cytoskeletal pattern. Compared to untreated cells, no change in the adhesion molecules was appreciated (Fig. 10b,d,f).

Cells on fibronectin were well spread, elongated or polygonal in shape, with several focal adhesions. At the focal adhesion sites the adhesive molecules were strongly stained, and vinculin clearly co-localised with actin (Fig. 11a,c,e). The cells without PCM were quite similar to untreated cells (Fig. 11b,d,f).

The focal contacts were also well organised on collagen-coated chambers. Paxillin and vinculin staining was prominent at the cell periphery, where they co-localise with actin. Actin stress fibres were also observed (Fig. 12c,e), while integrin $\beta 1$ was localised within the cytoplasm (Fig. 12a). Cells treated with hyaluronidase did not change their morphology. However, stress fibres were not organised, and paxillin was strongly reduced (Fig. 12b,d,f).

Discussion

In this paper, we analysed the role of PCM in the interaction of osteoblast-like cells with polyelectrolyte multilayers in order to investigate the early phases of cell attachment to a biomaterial substrate.

It is generally accepted that cells respond to a variety of surface-related features, such as chemistry, topography, wettability and stiffness, and integrate the resulting input to select behavioural pathways. Indeed, the early events of cell-substrate interaction, including changes in cell shape

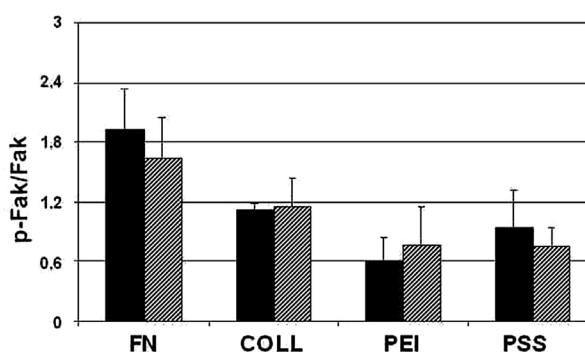
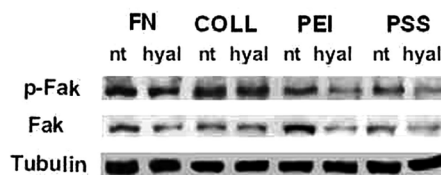


Fig. 7. Expression and activity of FAK protein at 6 h from cell seeding. (Top) Representative image of the western blot assay for FAK expression. Hyaluronidase treatment reduces the FAK protein expression, particularly on PEI (nt, non-treated cells; hyal, hyaluronidase-treated cells). (Bottom) FAK protein activity, calculated as phospho-FAK/total FAK ratio: the highest value is measured on fibronectin, while the lowest is recorded on PEI. The protein activity is not affected by hyaluronidase treatment. Mean \pm SEM. Black bars, untreated cells; striped bars, hyaluronidase-treated cells.

and cytoskeletal organisation, modulate short and long-term events, such as migration, proliferation, secretion and differentiation.

We used MG63 osteoblast-like cells as a model of PCM-coated cells. The thickness of the hyaluronan layer was indirectly detected by the erythrocyte exclusion assay, and a live-imaging technique using a glycosaminoglycan-specific fluorescent dye. To test if cells actually used negatively-charged PCM when adhering to a surface, cell morphology and adhesive structures during cell attachment, i.e. at 1, 3 and 6 h, were investigated. Cell shape and cytoskeletal organisation are good candidates to evaluate cell adhesion, since they are causally related to both long-term cell behaviour and substratum structure (Cretel *et al.*, 2008). In this study, we assumed that electrostatic forces would drive the early interaction of cells with synthetic substrates if the negatively charged hyaluronan-based PCM produces different cell behaviour respectively on a positively- or negatively-charged PEM surface. Likewise, the electrostatic interaction should affect cell behaviour if the charged hyaluronan-based PCM is efficiently removed. Two polyelectrolyte multilayers were constructed by the layer-by-layer method, giving a positively charged PEI and negatively charged PSS as terminal cell-facing layer. PEI is largely used as an initial layer for PEM deposition, thanks to its ability to provide a uniform anchoring network for the consecutive layers' formation (Kolasińska *et al.*, 2007). Minor cell toxicity has been reported for PEI (Brunot *et*

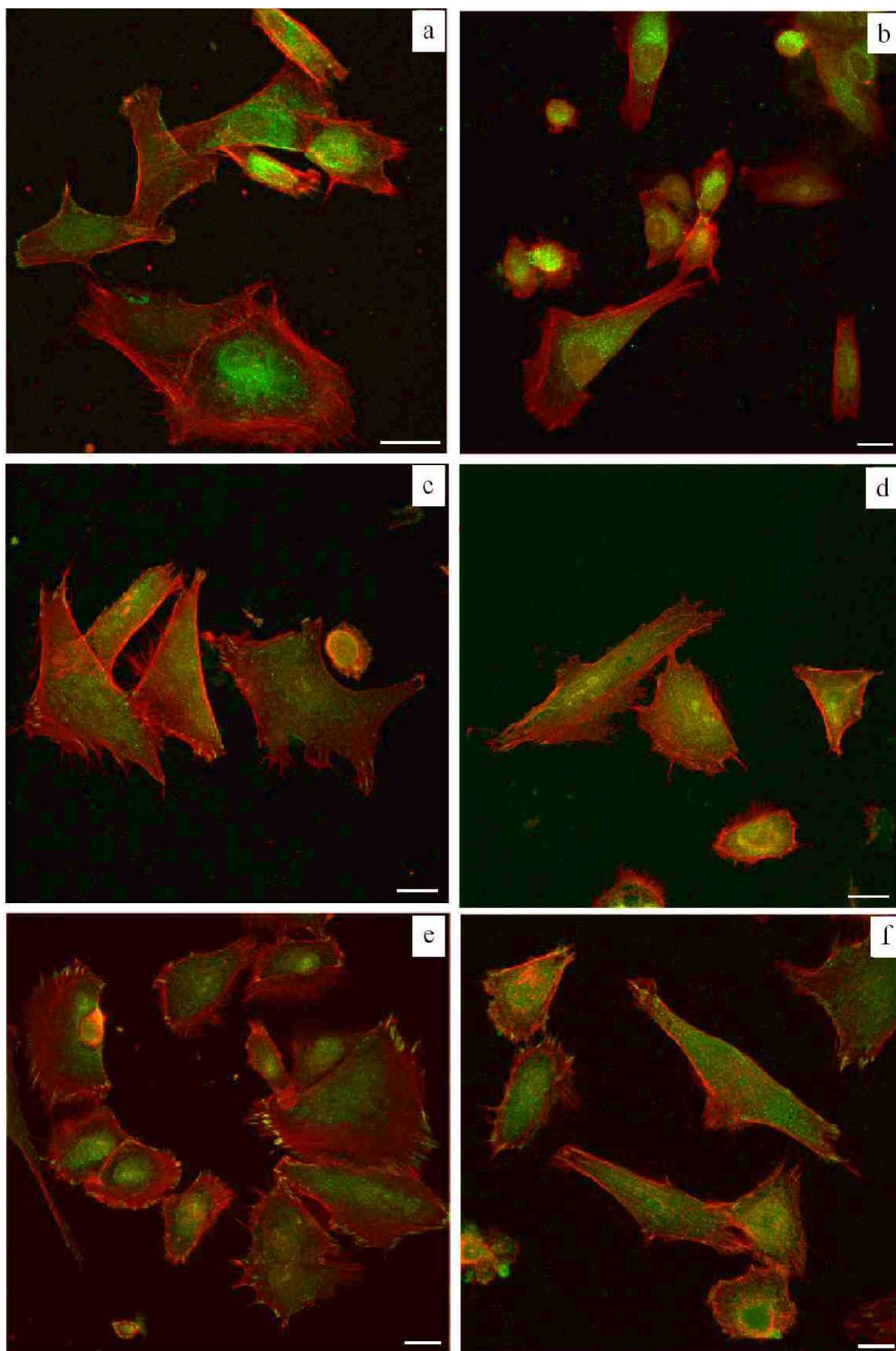


Fig. 8. Confocal image of MG63 cells on PSS, labelled for actin (red) and adhesion molecules (green), without (a, c, e) or with (b, d, f) hyaluronidase treatment. Adhesion molecules include integrin $\beta 1$ (a, b), paxillin (c, d) and vinculin (e, f). Cells show focal contacts with actin stress fibres, vinculin and paxillin clearly seen. After treatment with hyaluronidase the adhesion sites are few, without actin fibres and paxillin. Scale bar = 20 μm .

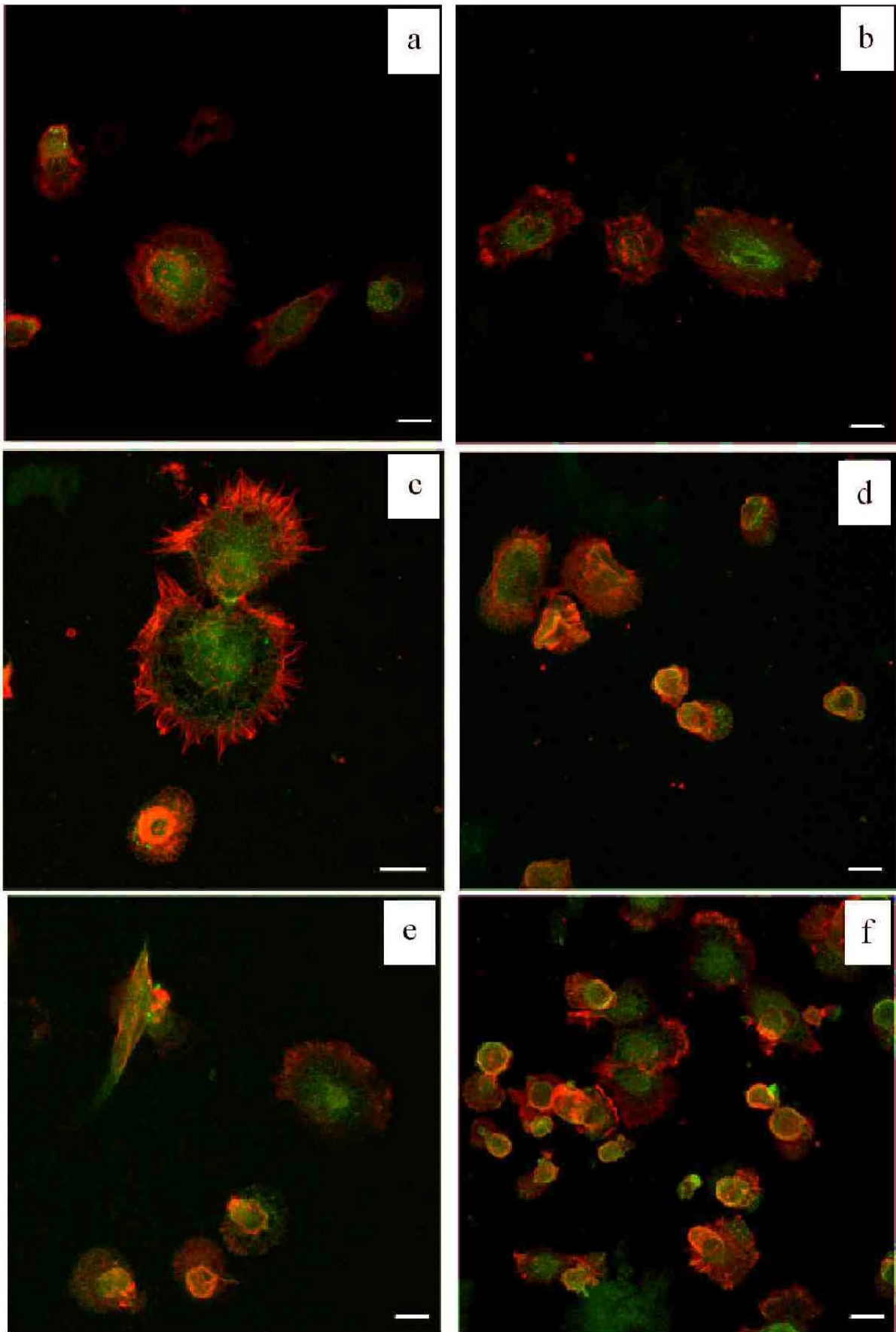


Fig. 9. Confocal image of MG63 cells on PEI, labelled for actin (red) and adhesion molecules (green), without (**a, c, e**) or with (**b, d, f**) hyaluronidase treatment. Integrin $\beta 1$ (**a, b**), paxillin (**c, d**) and vinculin (**e, f**). Actin is running at the cell edge and adhesion molecules are not organised in focal contacts. Pericellular matrix removal has no effect. Scale bar = 20 μm .

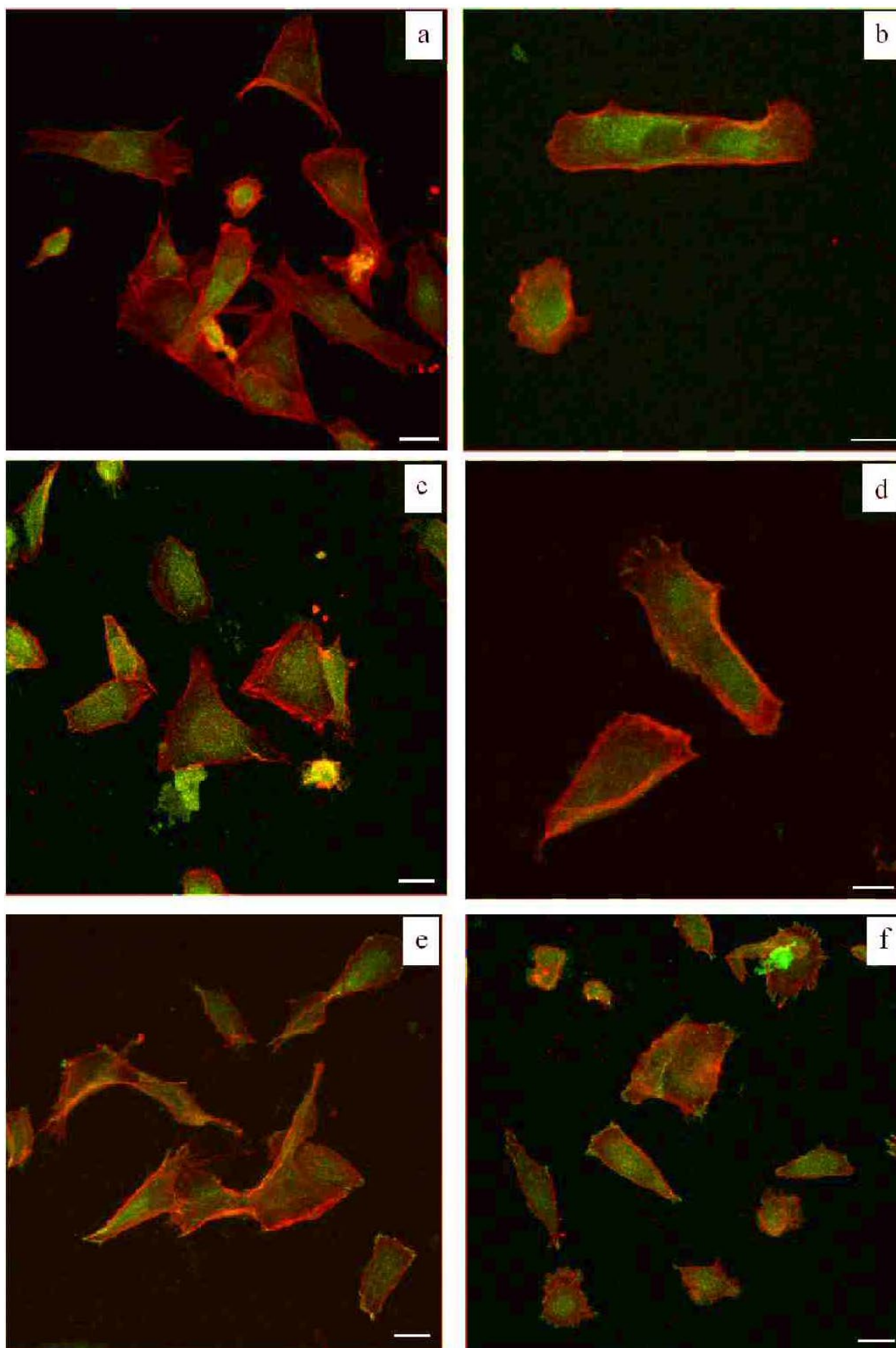


Fig. 10. Confocal image of MG63 cells on Permanox[®], labelled for actin (red) and adhesion molecules (green), without (a, c, e) or with (b, d, f) hyaluronidase treatment. Integrin $\beta 1$ (a, b), paxillin (c, d) and vinculin (e, f). Actin fibres and vinculin form late focal complexes, while no focal contacts are observed. After treatment with hyaluronidase the cytoskeleton is disrupted. Scale bar = 20 μm .

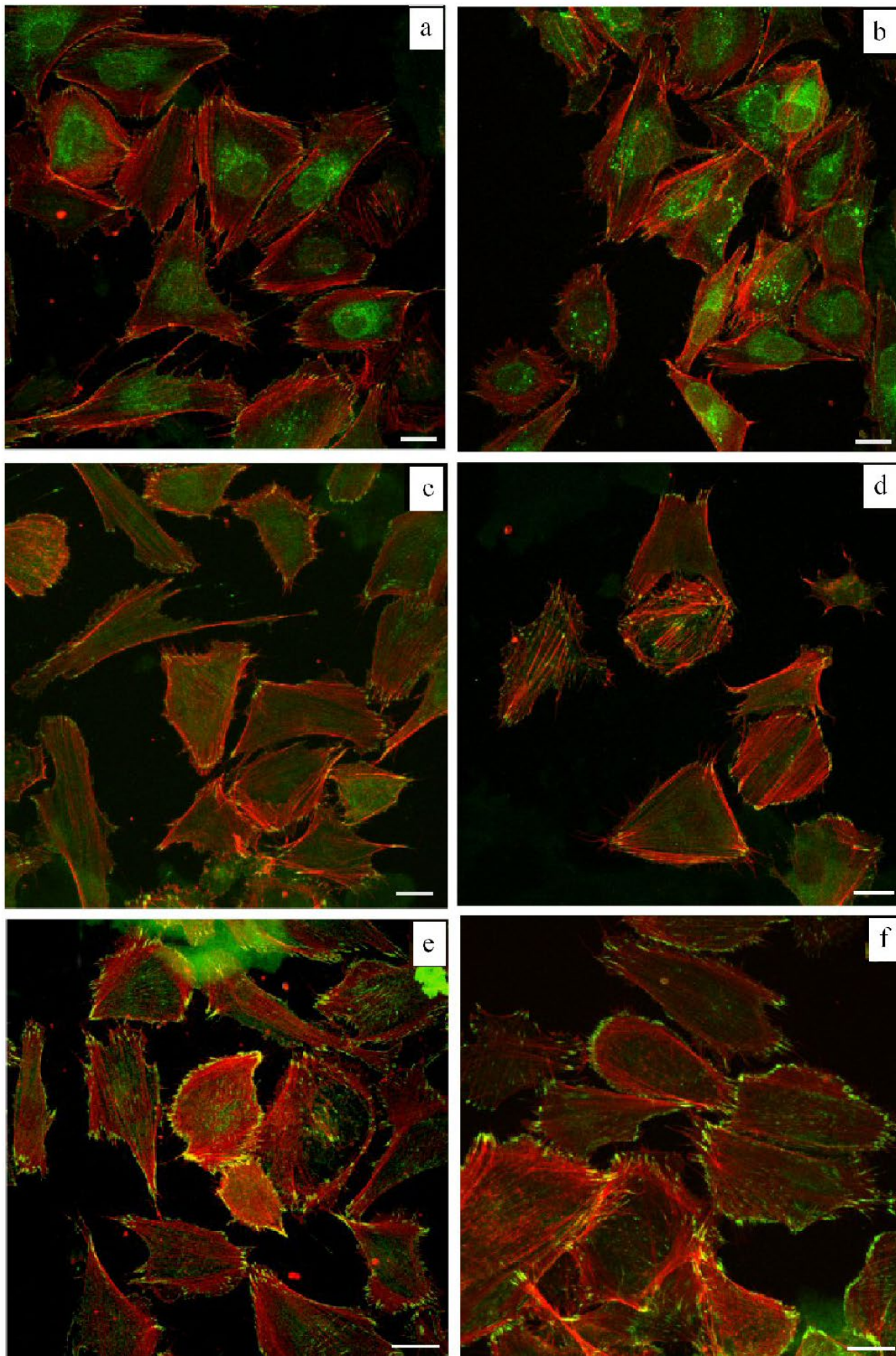


Fig. 11. Confocal image of MG63 cells on fibronectin, labelled for actin (red) and adhesion molecules (green), without (a, c, e) or with (b, d, f) hyaluronidase treatment. Integrin $\beta 1$ (a, b), paxillin (c, d) and vinculin (e, f). Cells form highly organised focal adhesions, with vinculin-actin co-localisation. After treatment with hyaluronidase no change is observed. Scale bar = 20 μm .

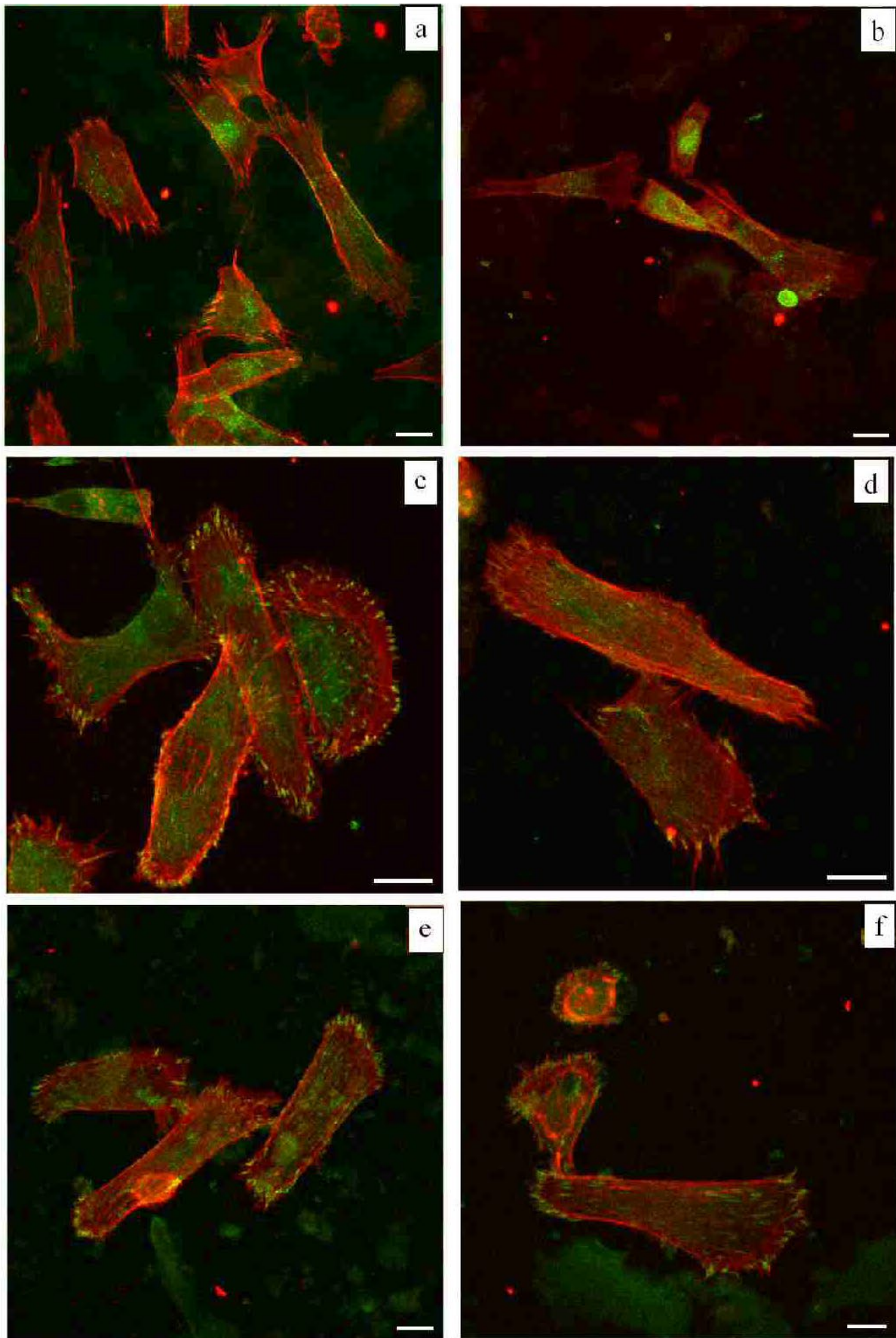


Fig. 12. Confocal image of MG63 cells on type I collagen, labelled for actin (red) and adhesion molecules (green), without (a, c, e) or with (b, d, f) hyaluronidase treatment. Integrin $\beta 1$ (a, b), paxillin (c, d) and vinculin (e, f). Focal contacts are seen, similar to those observed on PSS. After treatment with hyaluronidase the number of adhesion sites is reduced, with no stress fibres and organised paxillin. Scale bar = 20 μm .

al., 2007), partly dependent on the working concentration (Tryoen-Toth *et al.*, 2002) and the cell type. PSS is similarly compatible and currently used as a potassium-binding resin in hyperkalaemia (Inaba *et al.*, 2000).

Cells are highly mechanosensitive, and the assembly and disassembly of matrix adhesions are regulated in a dynamic fashion in response to cell signals and the exogenous tension provided by matrix rigidity/substrate stiffness (Berrier and Yamada, 2007). In our study, PEI and PSS films were quite thin ($\approx 3\text{--}5\ \mu\text{m}$), and the resulting stiffness was negligible in terms of cell response: if cells 'sense' the effective stiffness of rigid objects that are not in direct cellular contact, as shown by other authors (Buxboim *et al.*, 2010), in our experimental system the MG63 cells 'sensed' the stiff glass substrate underlying both PEM. Therefore any change of cell behaviour would be due to surface chemistry and/or charge.

The absence of movement of PEI-seeded cells, as seen by time-lapse microscopy, and the thick PCM layer adherent to the cell profile, observed by confocal microscopy at 3 h, suggested that PEI did not favour cell adhesion, despite its positive charge. MG63 cells on PEI showed a PCM similar to that observed a few minutes after seeding or just before detachment from a substrate, as in pre-mitotic cells, which show a dense accumulation of the pericellular matrix bordering the cell just before detachment and rounding (Cohen *et al.*, 2003; Evanko *et al.*, 1999). Indeed, it has been shown that if cell spreading is restricted, more round cells enter into apoptosis in comparison to spread cells (Re *et al.*, 1994).

We observed a tendency of PEI adherent cells to detach, particularly if deprived of their PCM. This phenomenon might be due to initial electrostatic PCM-PEI interactions, without further development of stable adhesion phenomena. Moreover, high levels of FAK protein expression did not correspond to an increased activity, and this expression was drastically reduced following PCM removal. Indeed, FAK phosphorylation, which mediates cell migration/proliferation, is sensitive to surface chemistry (Keselowsky *et al.*, 2004; Tilghman *et al.*, 2005). Consequently, the transition to more mature adhesion structures of cells loosely adherent to PEI substrate was inhibited or delayed.

A different behaviour was observed on the negatively-charged PSS surface, where MG63 cells actively moved under time-lapse microscopy, surrounded by a wide layer of PCM, as observed by confocal microscopy. By thickening along the flanks of locomoting cells, hyaluronan may provide a kind of lubrication along the plasma membrane/substrate interface, as suggested by another study (Turley and Torrance, 1984). PCM "footprints" were also detected, as described by others (Cohen *et al.*, 2003). The presence of active FAK protein further confirmed active cell mobility of PSS-seeded cells. Contrary to the expected repulsive effect of two anionic moieties (PSS and PCM), after PCM-mediated strong adhesion to PSS, cells started to spread and migrate, leaving remnants of their PCM – a pattern similar to that observed in cells seeded on fibronectin, the RGD-carrying substrate promoting cell adhesion and spreading. Even in PCM-deprived elements, the number of adherent cells on PSS did not change, while spreading and focal contact formation were slightly reduced. The failure

of the expected pattern of cell behaviour based on a simple electrostatic model suggests that the phenomenon of cell adhesion may be directly attributed to PSS, possibly due to the presence of acidic sulphonic groups of the PSS surface (Kowalczyńska *et al.*, 2003). The presence of "adhesion-effective" groups on PSS, such as the sulphonate moieties, would allow cells to bypass PCM in the attachment to the substrate, although, according to our results, PCM is still needed for the subsequent cell activities.

On fibronectin and type I collagen, the cells were observed to adhere and spread (von der Mark *et al.*, 2010). Fibronectin showed the highest values of cell adhesion, cell spreading and focal contact organisation, even after PCM removal.

On Permanox[®], a polyolefin treated for promoting cell attachment, rare MG63 cells were spread, with a thick PCM, as on PEI, and focal contacts were poorly organised. Following PCM removal, cell adhesion was significantly reduced. Hence, Permanox[®] is an unfavourable adhesion substrate, at least for these cells in the short term.

With regard to the charged surfaces, PEI- and PSS-based PEM were built using non-toxic concentrations of such polyelectrolytes, and their structure was analysed by AFM and XPS techniques. The XPS signals recorded are a convolution of the signals originating from the PEI and PSS layers in the films, as the XPS sampling depth for organic compounds is $\approx 10\ \text{nm}$ (Seah, 1980), and the film thickness is $\approx 3.0\ \text{nm}$ for PEI-PSS and $4.5\ \text{nm}$ for PEI-PSS-PEI.

As shown, PSS is predominant at the PEI/PSS surface ($\approx 60\%$ in normal take-off mode, up to 66% in surface-enhanced mode), while PEI prevails at the PEI/PSS/PEI surface, going from 76% to 85% . This means that the PEI/PSS/PEI film is terminated by a "pure" PEI layer, while at the PEI/PSS film surface the PSS component predominates, with a small contribution of PEI. Indeed, some entanglement of different polyelectrolyte chains may occur, producing partially mixed surfaces (Bucur *et al.*, 2006). The 'mixed' composition of the PSS-terminated PEM, with some PEI-areas, likely to reduce the electrical charge on PSS, does not affect the pro-adhesive ability of the sulphonic groups. This definitely indicates that the behaviour of MG63 cells on PSS- and on PEI-terminated PEM cannot be accounted for in terms of elementary electrostatic interactions.

In conclusion, we provided evidence for the role of the charged hyaluronan-based PCM in mediating interactions between cells and synthetic surfaces and regulating cell adhesion to charged PEM surfaces. Unexpectedly, osteoblast-like cells did not adhere to PEI, despite the electrostatic interaction between the negatively charged hyaluronan molecules and the positively charged groups on PEI. Similarly, negatively charged PSS surfaces exhibited a pro-adhesive activity, in spite of the expected repulsive interactions with negatively charged hyaluronan-based PCM. Surface chemistry therefore prevails over total surface charge in inducing cell adhesion to PEM, and confirms the wide potentiality of thin PEM films for the design of engineered ECM, where charge cues, chemical groups and nanoscale structure induce phenotypic cell modulation (Newcomer *et al.*, 2011).

Cell interaction with the external environment appears to be effectively mediated by PCM, playing as a sensor transducer triggering signalling events before integrin involvement (Cohen *et al.*, 2006). Such a “remote mechanosensitivity” model, through which cells “sense” the external matrix from a distance of a few μm and responds to it by activating adhesion and spreading, independently of the simple interaction of negative-to-positive forces, opens novel perspectives on the future design of surfaces for biomedical application.

Acknowledgements

G. Marletta gratefully acknowledges the partial financial support from PRIN 2010-2011, grant n.2010L9SH3k_002 (MIUR, Italy), and from FIRB Programme ITALNANONET, grant nr. RBPR05JH2P_22 (MIUR, Italy). We wish to confirm that there are no known conflicts of interest associated with this publication and there has been no significant financial support for this work that could have influenced its outcome.

References

- Berrier AL, Yamada KM (2007) Cell-matrix adhesion. *J Cell Physiol* **213**: 565-573.
- Bigerelle M, Anselme K (2005) Bootstrap analysis of the relation between initial adhesive events and long term cellular functions in human osteoblasts cultured on biocompatible metallic substrates. *Acta Biomater* **1**: 499-510.
- Briggs D, Seah MP (1990) Surface and interface characterization. In: Briggs D, Seah MP (eds) *Practical Surface Analysis*, volume 1, chapter 6. Wiley, Chichester.
- Brunot C, Ponsonnet L, Lagneau C, Farge P, Picart C, Grosgeat B (2007) Cytotoxicity of polyethyleneimine (PEI), precursor base layer of polyelectrolyte multilayer films. *Biomaterials* **28**: 632-640.
- Bucur CB, Sui Z, Schlenoff JB (2006) Ideal mixing in polyelectrolyte complexes and multilayers: entropy driven assembly. *J Am Chem Soc* **128**: 13690-13691.
- Buxboim A, Rajagopal K, Brown AEX, Discher DE (2010) How deeply cells feel: methods for thin gels. *J Phys Condens Matter* **22**: 194116.
- Cohen M, Klein ZE, Y Geiger B, Addadi L (2003) Organization and adhesive properties of the hyaluronan pericellular coat of chondrocytes and epithelial cells. *Biophys J* **85**: 1996-2005.
- Cohen M, Joester D, Geiger B, Addadi L (2004) Spatial and temporal sequence of events in cell adhesion: from molecular recognition to focal adhesion assembly. *Rev Chembiochem* **5**: 1393-1399.
- Cohen M, Kam Z, Addadi L, Geiger B (2006) Dynamic study of the transition from hyaluronan to integrin-mediated adhesion in chondrocytes. *EMBO J* **25**: 302-311.
- Cretel E, Pierres A, Benoliel AM, Bongrand P (2008) How cells feel their environment: a focus on early dynamic events. *Cell Mol Bioeng* **1**: 5-14.
- Entwistle J, Hall CL, Turley EA (1996) HA receptors: regulators of signalling to the cytoskeleton *J Cell Biochem* **61**: 569-577.
- Evanko SP, Angello J, Wight T (1999) Formation of hyaluronan and versican rich pericellular matrix is required for proliferation and migration of vascular smooth muscle cells. *Arterioscler Thromb Vasc Biol* **19**: 1004-1013.
- Finke B, Luethen F, Schroeder K, Mueller PD, Bergemann C, Frant M, Ohl A, Nebe BJ (2007) The effect of positively charged plasma polymerization on initial osteoblastic focal adhesion on titanium surfaces. *Biomaterials* **28**: 4521-4534.
- Finšgar M, Fassbender S, Hirth S, Milošev I (2009) Electrochemical and XPS study of polyethyleneimines of different molecular sizes as corrosion inhibitors for AISI 430 stainless steel in near-neutral chloride media. *Mater Chem Phys* **116**: 198-206.
- Inaba S, Nibu K, Takano H, Maeda Y, Uehara K, Oshige T, Yuasa T, Nakashima H (2000) Potassium-adsorption filter for RBC transfusion: a phase III clinical trial. *Transfusion* **40**: 1469-1474.
- Keselowsky BG, Collard DM, Garcia AJ (2004) Surface chemistry modulates focal adhesion composition and signaling through changes in integrin. *Biomaterials* **25**: 5947-5954.
- Knudson CB, Knudson W (1993) Hyaluronan-binding proteins in development, tissue homeostasis, and disease. *FASEB J* **7**: 1233-1241.
- Kolasińska M, Krastev R, Warszyński P (2007) Characteristics of polyelectrolyte multilayers: Effect of PEI anchoring layer and posttreatment after deposition. *J Colloid Interf Sci* **305**: 46-56.
- Kowalczyńska HM, Nowak-Wyrzykowska M (2003) Modulation of adhesion, spreading and cytoskeleton organization of 3T3 fibroblasts by sulfonic groups present on polymer surfaces. *Cell Biol Int* **27**: 101-114.
- Lee GM, Johnstone B, Jacobson K, Catterson B (1993) The dynamic structure of the pericellular matrix on living cells. *J Cell Biol* **123**: 1899-1907.
- Mitra SK, Hanson DA, Schlaepfer DD (2005) Focal adhesion kinase: in command and control of cell motility. *Nat Rev Mol Cell Biol* **6**: 56-68.
- Newcomer RG, Moussallem MD, Keller TC, Schlenoff JB, Sang QX (2011) Human coronary artery smooth muscle cell responses to bioactive polyelectrolyte multilayer interfaces. *Biotechnol Res Int* **2011**: 854068.
- Niepel MS, Peschel D, Groth T (2011) Controlling fibroblast adhesion with pH modified polyelectrolyte multilayers. *Int J Artif Organs* **34**: 185-191.
- Popat KC, Sharma S, Desai TA (2004) Quantitative XPS analysis of PEG-modified silicon surfaces. *J Phys Chem B* **108**: 5185-5188.
- Re F, Zanetti A, Sironi M, Polentarutti N, Lanfrancone L, Dejana E, Colotta F (1994) Inhibition of anchorage-dependent cell spreading triggers apoptosis in cultured human endothelial cells. *J Cell Biol* **127**: 537-546.
- Santos JP, Welsh ER, Gaber BP, Singh A (2001) Polyelectrolyte-assisted immobilization of active enzymes on glass beads. *Langmuir* **17**: 5361-5367.
- Seah M (1980) The quantitative analysis of surfaces by XPS: A review. *Surf Interf Anal* **2**: 222-239.

Stern R (2003) Devising a pathway for hyaluronan catabolism: are we there yet? *Glycobiology* **13**: 105R-115R.

Suzuki Y, Kusakabe M, Iwaki M, Suzuki M (1988) Surface modification of silicone rubber by ion implantation. *Nucl. Instrum Methods Phys Res B* **32**: 120-124.

Tilghman RW (2005) Focal adhesion kinase is required for the spatial organization of the leading edge in migrating cells. *J Cell Sci* **118**: 2613-2623.

Ting JH, Haas MR, Valenzuela SM, Martin DK (2010) Terminating polyelectrolyte in multilayer films influences growth and morphology of adhering cells. *IET Nanobiotechnol* **4**: 77-90.

Tryoen-Toth P, Vautier D, Haikel Y, Voegel JC, Schaaf P, Chluba J, Ogier J (2002) Viability, adhesion, and bone phenotype of osteoblast-like cells on polyelectrolyte multilayer films. *J Biomed Mater Res* **60**: 657-667.

Turley EA, Torrance J (1984) Localization of hyaluronate and hyaluronate binding protein on motile and non-motile fibroblasts. *Exp Cell Res* **161**: 17-28.

von der Mark K, Park J, Bauer S, Schmuki P (2010) Nanoscale engineering of biomimetic surfaces: cues from the extracellular matrix *Cell Tissue Res* **339**:131-153.

Zimmerman E, Geiger B, Addadi L (2002) Initial stages of cell-matrix adhesion can be mediated and modulated by cell-surface hyaluronan. *Biophys J* **82**: 1848-1857.

Discussion with Reviewer

Reviewer II: Do the authors think that PCM/material interactions could be important in stem cell differentiation regulation as seen with the role of adhesions in response to stiffness, chemistry and topography?

Authors: We think that PCM could play a role in stem cell differentiation, as this process is strongly dependent on bridging between the cell surface and substrate with subsequent 'mechanotransduction'.

In a recent paper on MSC response to substrate stiffness, a first phase of cell adhesion where '...the cell adheres passively and starts to sense the substrate' is reported (Tam *et al.*, 2012). In our opinion, this 'passive adhesion' step is coincident with the PCM/surface phase of interaction, which could not be as passive as it appears.

Indeed, this biological structure is able to escape some simple theoretical rules, such as positive-to-negative electrostatic interaction, as shown in the present work. Likewise, PCM could modulate other cell activities.

A recent paper by Darzynkiewicz and Balazs (2012) shows that the expression of hyaluronan (HA) on the cell surface correlates with the differentiation status of stem and progenitor cells, with the highest HA expression observed on the surface of the most primitive (Lin-) stem cells, and a progressive decline seen to be concurrent with differentiation.

Finally, Mathieu and Lobo (2012) have found that '...osteogenic differentiation is prevalent in MSCs with a stiff, spread actin cytoskeleton and greater numbers of focal adhesions, while adipogenic or chondrogenic differentiation are encouraged when MSCs have a spherical morphology associated with a dispersed actin cytoskeleton with few focal adhesions'. Since from our study and others, PCM apparently modulates the formation of adhesive structures, it may be included in the mechanisms/structures that stand upstream to stem cell differentiation process.

In conclusion, PCM/substrate interaction may be a determinant in mesenchymal stem cells biology, as the cell employs PCM to 'contact' the surface, then the material surface features dictate the PCM organisation, which in turn affects cytoskeletal actin, adhesive structures and cell spreading, required for subsequent cell migration/differentiation.

Additional References

Tam JKC, Uto K, Ebara M, Pagliari S, Forte G, Aoyagi T (2012) Mesenchymal stem cell adhesion but not plasticity is affected by high substrate stiffness. *Sci Technol Adv Mater* **13**: 064205.

Darzynkiewicz Z, Balazs EA (2012) Genome integrity, stem cells and hyaluronan. *Aging* **4**: 78-88.

Mathieu PS, Lobo EG (2012) Cytoskeletal and focal adhesion influences on mesenchymal stem cell shape, mechanical properties, and differentiation down osteogenic, adipogenic, and chondrogenic pathways. *Tissue Eng Part B* **8**: 437-444.